A Study of the Slowing Down Distribution of Sb^{124}-Be Photo-Neutrons in Graphite, and of the Use of Indium Foils*

L. D. ROBERTS, J. E. HILL, AND G. MCCAMMON
Oak Ridge National Laboratory, Oak Ridge, Tennessee

(Received May 1, 1950)

The spatial density distribution of indium resonance neutrons (1.44 ev resonance) has been measured around a point Sb^{124}—Be photo-neutron source in a graphite slowing down medium. This distribution was found to be in agreement with appropriate theory. The source energy of the photo-neutrons was calculated from the measured neutron distribution and a value of 20 ± 4 kev was obtained in fair agreement with values obtained by other methods. It was found that there is a quite appreciable capture cross section in In^{115} above the 1.44-ev resonance extending in energy to at least several kev. It is shown that this capture of neutrons with energies above 1.44 ev can introduce an error into neutron slowing down measurements which can be important under some circumstances, and it is shown how this error can be corrected.

I. INTRODUCTION

FAST neutrons, emitted from a point source in a medium of infinite extent and of atomic weight large compared with the neutron mass, slow down in such a way as to give a spatial neutron density distribution of slower neutrons (of 1.44 ev energy, for example) which is approximately gaussian. It seems that this first approximation to the spatial neutron density distribution was first used some time ago by Bethe, Korff, and Placzek[1] in their investigation into the slowing down of cosmic-ray neutrons in the atmosphere. More recently, Placzek[2] and Marshak[3] have obtained theoretically the next approximation to this neutron density distribution. Although many neutron slowing down density distribution measurements have been made, the experimental conditions in all of these have always been so complex that this theoretical treatment was not directly applicable. We have performed an experiment under such conditions that the theoretical treatment applies quite well. Our measurement served the following purposes. First, by fitting the measured neutron density distribution to Placzek's theoretical distribution a parameter was obtained from which we calculated the energy of the photo-neutrons produced by the interaction of Sb^{124} gamma-rays with Be. Second, it was possible to study the errors in the use of indium foils for epithermal neutron flux measurements. One possible error, pointed out to us by Dr. G. Goertzel, may arise as follows. From the work of Havens *et al.*[4] and Segrè[5] it is known that indium has a total cross section of the order of thirty barns extending up into the kilovolt energy region with an appreciable fraction of this due to capture. On the other hand it is usually assumed that only the 1.44-ev indium resonance contributes appreciably to the indium foil activity when the latter is used for epithermal neutron flux measurements, as in the measurement of a neutron slowing down distribution. Considering the fact that the 1.44-ev resonance will be quite strongly self-protected in a foil of usual thickness ($\sim$0.1 g/cm^2), it is clear that any part of the above 30 barns caused by capture may be relatively important in the interpretation of the foil activity as a neutron flux at resonance energy.

In the course of the following discussion we shall show that, for gaussian slowing down, and with a neutron source energy as low as ours, about 24 kev, neutron capture at energies above 1.44 ev does contribute to the indium foil activity, and if this additional activity should be interpreted as due to the 1.44-ev resonance, an appreciable error would result in the spatial neutron density distribution. Another case in which capture above 1.44 ev would be important would be that in which the neutron energy spectrum contained a high proportion of neutrons in the kilovolt energy region relative to the proportion in the 1 to 10 volt energy region. We shall not treat this case, however.

II. EXPERIMENTAL EQUIPMENT AND TECHNIQUE

(A) The Neutron Source

From the recent work of Meyerhof and Scharff-Goldhaber,[6] it is found that Sb^{124} has but one gamma-ray capable of producing photo-neutrons in beryllium, neglecting a small percentage of cross-over transitions. Wattenberg,[7] and Hanson and Hemmendinger[8] have found Sb^{124}+Be to be a very satisfactory source of photo-neutrons of about 24 kev energy. Because of the low monochromatic energy of the neutrons, which would emphasize the effect of capture in the kilovolt energy region; and because there has been some disagreement in the literature concerning the energy of Sb^{124}—Be photo-neutrons (which energy our experiment would measure) we selected this combination as our neutron source.

* This document is based on work performed for the Atomic Energy Project at Oak Ridge National Laboratory.
[1] Bethe, Korff and Placzek, Phys. Rev. **57**, 573 (1940).
[2] G. Placzek, Manhattan Project Report A-25 (unpublished).
[3] R. E. Marshak, Rev. Mod. Phys. **19**, 212–213 (1947).
[4] Havens, Wu, Rainwater, and Meaker, Phys. Rev. **71**, 165 (1947).
[5] E. Segrè, Rev. Mod. Phys. **19**, 283 (1947).
[6] W. E. Meyerhof and G. Scharff-Goldhaber, Phys. Rev. **72**, 273 (1947).
[7] A. Wattenberg, Phys. Rev. **71**, 497 (1947).
[8] A. O. Hanson and A. Hemmendinger, Phys. Rev. **75**, 1794 (1949).

The source consisted of a sphere of normal antimony about 1.59 cm in diameter and weighing 13.6 g enclosed in a spherical beryllium shell with an over-all diameter of about 2.5 cm and weighing 9.24 g. The antimony sphere was activated in the Oak Ridge National Laboratory pile.

Because of their smaller mass, beryllium atoms are more effective than are carbon atoms in slowing down neutrons. The amount of beryllium in our source, however, was too small to perturb the neutron flux distribution in the slowing down medium detectably. This was demonstrated by measuring two neutron flux distributions, one with the neutron source described above, and one with a source containing approximately 0.1 as much beryllium, i.e., (0.963 g). The ratio between the two distributions, shown in Table I, columns 4 and 5, was independent of the distance from the source, being constant to within one percent, thus demonstrating the fact that the beryllium in the neutron source did not perturb the measured neutron distribution.

(B) The "Slowing-Down" Medium

The slowing-down medium which we selected was graphite. This was used because graphite has a constant and fairly small scattering cross section from 1 ev to $\sim$100 kev. This is illustrated by Table II. A simple average of these values gives $\bar{\sigma}_s = 4.59\times 10^{-24}$ cm^2. Also, the ratio of the mass of C^{12} to the neutron mass is sufficiently large that one might expect the Placzek distribution to apply.

The graphite column in which the experiments were made had an average density of 1.652 g/cm^3 and the dimensions were 6 ft.$\times$6 ft.$\times$11 ft. The neutron source was located at the center of this column and the neutron flux measurements were made along the central 11 ft. or principal axis. The graphite column dimensions were such that it was effectively infinite in size for our neutron source and detection energies.

(C) Neutron Flux Measurements

We were interested in measuring the isotropic component of the neutron flux at a particular resonance energy and at a number of positions along the principal axis of the graphite column. To do this, indium foils suitably protected from the thermal flux by cadmium, or from the thermal and slightly higher energy flux by B^{10} or from thermal and resonance energy flux by cadmium plus indium self-protection, were activated at the desired positions in the column for approximately eight half-lives and then counted on both sides. During the activation the foils were oriented in the plane perpendicular to the principal axis of the column. The saturated activity, i.e., the foil activity immediately after an infinite time of activation, was then calculated for each side of the foil using 54 min. as the half-life of indium and the average of these two values, $A_s(r, u)$, (Section IIIA) was obtained. It is this average saturation activity $A_s(r, u)$ which is proportional to the isotropic component of the neutron flux.[9] The foils were usually counted one or two half-lives to obtain the best possible statistics. Also, the results reported in Table III represent the average of many experiments. The counting was done on a thin-wall glass β-ray counter connected to a scale of 64.

All of the foils were 4 cm$\times$6.35 cm in area, the indium foils being 0.094 ± 0.0005 g/cm^2 thick. The cadmium boxes in which the foils were encased were about 2.9 g/cm^2 thick. When B^{10} was used, it was in the form of a powder assaying 98 percent in boron of which 90 percent was B^{10}. The boron powder was used by packing it in a box of such design that the foil was completely enclosed with a uniform layer of boron, but of such a shape that the boron was essentially undisturbed from one experiment to another. The thickness of the boron layer was either 0.338 g/cm^2 or 1.334 g/cm^2.

We were not interested in the absolute value of the neutron flux but only in quantities proportional to this. Hence, we report simply the saturated activity of the foil $A_s(r, u)$ and not the corresponding neutron flux which produced the activity.

It should be mentioned that an experiment was made to see whether the antimony gamma-rays would activate the foils. No activity was found.

(D) Geometrical Corrections

It is an interesting fact that if the spatial distribution to be measured has a Gaussian form, a spherical shell source of finite size will appear as a point source if the detector is close to the source. Similarly, a detector of finite size will appear as a point detector. This will perhaps be made clear by the following discussion.

Consider a source which is a spherical shell of radius α with a point detector on the r axis at position r_0. Then, with τ a constant defined in Section IIIA, the flux at r_0 will be approximately proportional to the integral

$$nv(r_0, \tau) \sim 2\pi \int_0^{\pi} \sin\theta d\theta \exp(-\rho^2/4\tau). \qquad (1)$$

Substituting $\rho^2 = \alpha^2 + r_0^2 - 2r_0\alpha \cos\theta$ and integrating we find

$$nv(r_0, \tau) \sim 4\pi\alpha \left(\frac{2\tau}{\alpha r_0}\right) \sinh\left(\frac{\alpha r_0}{2\tau}\right) \exp\left[-\frac{\alpha^2 + r_0^2}{4\tau}\right]. \qquad (2)$$

TABLE I. Neutron flux distributions with different sources.

r (cm)	A_s (9.241 g source)	A_s' (0.963 g source)	$A_s'\times(17.506)$	$100(A - A_s'\times 17.506)/A_s$ percent dev.
7.78	3081	176.0	3081	——
12.86	2358	134.8	2360	+0.08
17.94	1654	94.34	1652	−0.12
23.02	1123	63.95	1120	−0.27

[9] W. Bothe, Zeits. f. Physik **120**, 437–449 (1943).

TABLE II. The scattering cross sections of graphite from 1.10 ev to 95 kev.

Energy	Scattering cross section	Reference
1.10 ev	4.45 barns	a
1.44	4.84	b
2.00	4.50	a
5.00	4.43	a
24 kev	4.6	c
35	4.63 ± 0.19	d
95	4.65 ± 0.14	d
	Av. 4.59 barns	

[a] Goldsmith, Ibser, and Feld, Rev. Mod. Phys. **19**, 266 (1947), see Fig. 11.
[b] J. Marshall, Phys. Rev. **70**, 107 (1946).
[c] Wattenberg, Fields, Russell, and Sachs, Phys. Rev. **71**, 508 (1947).
[d] D. H. Frisch, Phys. Rev. **70**, 589 (1946).

If $\alpha r_0/2\tau \leqslant 0.25$, $\sinh(\alpha r_0/2\tau) \cong \alpha r_0/2\tau$ to within 1 percent. Making this substitution we get

$$nv(r_0, \tau) \sim 4\pi\alpha \exp[-(\alpha^2 + r_0^2)/4\tau], \tag{3}$$

which is Gaussian in r_0. In this experiment $\tau = 147$ cm^2, $\alpha \cong 1.25$ cm, so that the maximum value of r_0 allowed by the above criterion would be $r_0(\max) = 60$ cm. Our measurements lie within this range. The proof that a detector of finite size will appear as a point detector in a Gaussian flux distribution is similar to the above. The deviation of the theoretical distribution[2, 3] from a Gaussian form is small and does not need to be taken into account in the above considerations of geometry corrections. Thus, our experimental conditions correspond very closely to an ideal point geometry.

III. EXPERIMENTAL RESULTS

(A) Fit of Data to the Theoretical Distribution

In our experiment, we have measured the saturation activity of an indium foil $A_s(r, u)$ measured in β counts/min. as a function of distance r of the foil from the neutron source and corresponding to the logarithmic neutron energy u. The major part of the indium foil activity will be due to the narrow region of logarithmic energy, u, at the 1.44-ev indium resonance. This measured function, A_s, should be proportional to the theoretical slowing down density distribution and thus we write,[2, 3]

$$\underset{\text{(measured)}}{A_s(r, u)} = c\frac{\exp(-r^2/4\tau)}{E_d \tau^{3/2}}\left[1 + \frac{F(r^2/\tau)}{4u}\right], \tag{4}$$

where r is the source to foil distance in cm, c is a constant, the logarithmic energy $= u = \ln(E_s/E_d)$, E_s is the source energy in volts, E_d is the energy in volts at which the neutrons are detected, i.e., captured, and $\tau = \lambda_s^2 u/K$ where λ_s is the neutron scattering mean free path in graphite and K is a constant depending on the masses of C^{12} and of the neutron.[2, 3] The coefficients in $F(r^2/\tau)$ below also depend simply on the masses of C^{12} and of the neutron.[2, 3]

$$F(r^2/\tau) = 2.68599 - 1.16432(r^2/\tau) + 0.071665(r^2/\tau)^2.$$

The function $A_s(r, u)$ measured with cadmium covered indium detectors is given in Table III, column A. The graph, Fig. 1, shows a plot of these experimental points on the coordinates $\ln_{10} A_s$ *vs.* r^2 which for a

TABLE III. Neutron flux measurements.

Distance of foil from neutron source		*A* Measured saturated activity of In foil covered with Cd only		*B* Measured saturated activity of In foil covered with Cd and with three different thicknesses of In. Thickness in cm			*C* Column *A* saturated activities corrected for high energy components by use of column *B* for the three In thicknesses in cm			*D* Average of column *C* (corrected)	
r	r^2	$A_s(r, u)$	$\ln_{10} A_s(r, u)$	0.0127	0.0254	0.0508	0.0127	0.0254	0.0508	$A_s(r, u)$	$\ln_{10} A_s(r, u)$
3.551	12.61	3529	3.54770	1650	1308	1052	3155.3	3035.4	2972.2	3054.4	3.48493
6.091	37.10	3162	3.50001	1411	1101	839.5	2940.4	2816.7	2787.1	2848.1	3.45455
8.631	74.49	2836	3.45271	1220	935.0	679.6	2713.7	2598.05	2587.8	2633.2	3.42065
11.171	124.79	2563	3.40870			585.2			2373.5	2373.5	3.37535
13.71	187.96	2240	3.35017			486.5			2104.3	2104.3	3.32311
16.25	264.06	1906	3.28007								
18.79	353.06	1581	3.19896	630.6	440.4	316.1	1596	1558.8	1517.9	1557.6	3.19246
21.33	454.97	1276	3.10584								
23.02	529.9	1122.8	3.05030								
23.82	567.4	1051.2	3.02168			178.87			1046.8		3.01987
28.10	789.6	711.3	2.85205								
28.90	835.20	656.3	2.81713			109.85			655.8		2.81677
33.18	1100.9	410.8	2.61363								
33.98	1154.6	373.8	2.57262			57.74			379.3		2.57898
38.26	1463.8	217.0	2.33646								
39.04	1524.1	197.4	2.29542	79.85	52.97	34.54			195.4		2.29092
43.34	1878.4	113.3	2.05423								
48.42	2344.5	52.09	1.71675								
49.27	2427.5	47.67	1.67822								
53.50	2862.3	26.65	1.42570								
54.35	2953.9	21.50	1.33245								
58.58	3431.6	12.08	1.08207								
59.43	3531.9	10.17	1.00746								
63.66	4052.6	4.84	0.68485								

simple Gaussian form on these coordinates would be a straight line. The best fitting straight line, $\tau = 147$ cm^2, is dotted in Fig. 1, to show the departure of the experimental data from this first approximation. The deviation is about a factor of 2 at our largest value of r. The solid curve drawn through the experimental points is the best fit of the second theoretical approximation, Eq. (4), using $\tau = 147$ cm^2. From $r^2 = 400$ cm^2 to $r^2 = 4000$ cm^2, the fit is seen to be quite good, but between $r^2 = 0$ and $r^2 \cong 400$ cm^2 the experimental points fall significantly above the theoretical curve. These two regions of r will be discussed separately below.

(B) Calculation of the Energy of Sb^{124}-Be Photo-Neutrons

We have taken the value of the carbon scattering cross section in the relevant energy range as 4.59×10^{-24} cm^2, Table II. For our graphite density of 1.652 g/cc, this gives $\lambda_s = 2.63$ cm. Referring to the definition of τ, Eq. (4), one can then calculate the logarithmic energy u. Taking the 1.44-ev line $= E_d$ and $\tau = 147$ cm^2, one obtains the source energy, $E_s = 20$ kev. The probable error of τ/λ_s^2 is perhaps of the order of 2 percent. This leads to an error of about 20 percent in E_s. Within this error there is agreement with the previous result of $\sim$24 kev found by Wattenberg, and by Hansen and Hemmendinger (see reference b, Table II). Due to self-protection the effective value of E_d is somewhat less than 1.44 ev but considering the above error it is not worthwhile to make this refinement.

(C) Activation of Indium in the Energy Range Above 1.44 ev and the Effect of This Activation on Foil Measurements

As was noted above, Eq. (4) fits the experimental data very well from $r^2 = \sim 400$ cm^2 to $r^2 = 4000$ cm^2 (Fig. 1), but, as is shown clearly upon examination of the graph, the experimental points fall far above this theoretical curve near the origin. The first point at $r^2 = 12.61$ cm^2 is about 16 percent higher than the theoretical value, (Eq. (4)). Since one would expect the theory to be best in the region of small r, it would seem that there must be some additional phenomenon occurring. As mentioned earlier, although beryllium has a greater slowing down effect than graphite, we were able to show that the quantity of beryllium used even if reduced by almost a factor of 10 made no measurable change in the distribution in Table III. Thus the anomaly could not be due to the neutron source.

Also, this anomalous distribution could not be due to geometrical corrections or to γ-ray activation of the indium, as was mentioned earlier.

This additional activity at small r can be understood, however, when one recalls that indium has an appreciable total cross section[4, 5] up to several kev, and that an appreciable part of this is due to capture. In Section IIIB we noted that the value of $\tau = 147$ cm^2 was equivalent to an energy, $E_d = 1.44$ ev, at which the majority of the neutrons were captured by the foil over the distribution of A_s *vs.* r. Close to the neutron source, however, the neutron flux is especially rich in neutrons with energies in the kilovolt region, and these higher energy neutrons may be captured by the detecting foil. Now capture at energies higher than 1.44 ev will correspond to $\tau < 147$ cm^2 causing $\exp(-r^2/4\tau)$ to fall off faster than for the principal value of τ, 147 cm^2. If then a theoretical $A_s(r, u)$ be composed of two parts, a major part caused by the function (Eq. (4)) with $\tau = 147$ cm^2, and a second smaller part consisting of a suitable integral over this function for a spectrum of $\tau < 147$ cm^2, our experimental data may be fitted. The correctness of this explanation that the additional activity is due to neutron capture by the foil at energies above 1.44 ev may be demonstrated by using indium self-absorption and boron absorption experiments.

(D) Self-Absorption Experiments

These measurements were made by enclosing the detecting indium foil with the usual cadmium box and with a box made from indium in addition. Three different wall thicknesses of the indium were used in experiments with the additional indium box, 0.005 inch, 0.010 inch, and 0.020 inch. Reference to Fig. 1 shows that the measured points, cadmium covering only, fit the theoretical curve with but a single $\tau = 147$ cm^2 beyond $r^2 \cong 350$ cm^2. It is assumed then that the foil activity is essentially due to the 1.44-ev resonance at and beyond this value of r^2. Thus a self-absorption experiment made at r^2, about 353 cm^2, would correspond to the 1.44-ev line only. The 3.8-ev and 8.6-ev lines do not lead to the 54-min. activity.[10] On the other hand, a self-absorption measurement made at r^2 about 12 cm^2 would consist of two parts, the higher energy part in which the indium cross section is small compared with the 1.44-ev resonance, and for which essentially no self-absorption would occur, plus the activity of the 1.44-ev line, which would be self-absorbed in the same

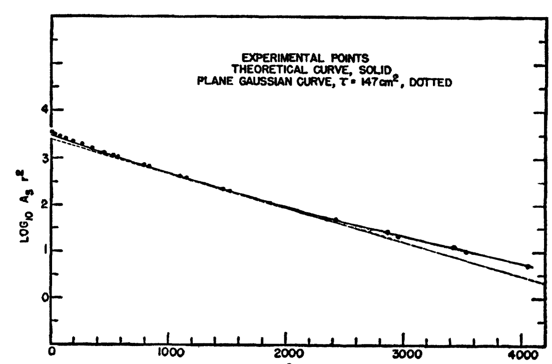

FIG. 1. Data on the neutron density distribution from a spherical shell source.

[10] M. Goldhaber (private communication).

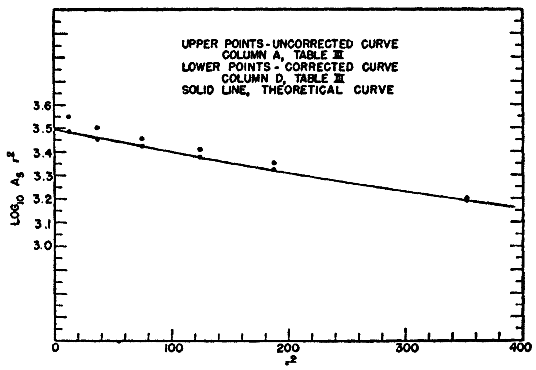

FIG. 2. Comparison of the corrected experimental values with the theoretical distribution.

way as at $r^2=353$ cm^2. Then the saturated activities for foils covered only with cadmium, are

$$A_{\text{Cd}}(12.61\text{ cm}^2)=\underset{\text{(1.44 ev line)}}{A_s(r_1, u)}+A(\text{high energy}), \quad (5)$$

$$A_{\text{Cd}}(353.1\text{ cm}^2)=\underset{\text{(1.44 ev line)}}{A_s(r_2, u)} \quad (6)$$

and the saturated activities for foils covered with both camium and indium

$$A_{\text{Cd+In}}(12.61\text{ cm}^2)=\underset{\text{(lines)}}{A_s(r_1, u)}\cdot F+A(\text{high energy}), \quad (7)$$

$$A_{\text{Cd+In}}(353.1\text{ cm}^2)=\underset{\text{(lines)}}{A_s(r_2, u)}\cdot F, \quad (8)$$

where F is the factor of self-absorption assumed independent of r of the 1.44-ev line by the indium.

By measuring A_{Cd} and $A_{\text{Cd+In}}$ in (5), (6), (7) and (8), one can solve these simultaneously and obtain F, $A_s(r, u)$, and A(high energy). We are primarily interested in calculating $A_s(r, u)$; i.e., in correcting the experimental curve for the high energy component. This has been done at ten foil positions and for three thicknesses of indium absorber. The same Cd thickness was used in all cases. Note, in column C, Table III, the good agreement for the three indium thicknesses. The agreement between the theory (Eq. (4)), and this corrected experimental A_s, column D, Table III, is shown in Fig. 2 and is seen to be very good.

TABLE IV. Boron absorption measurements.

r	0.338 g/cm^2 boron	1.334 g/cm^2 boron
3.551	309.1	191.6
6.091	169.0	98.9
8.631	100.2	59.5
11.171	66.4	35.1
13.71	27.4	14.5
16.25	20.5	8.9
18.79	13.0	

Thus, it is shown that the anomalous activity is due to a comparatively low cross section in the indium of comparatively high mean energy, and it is clear that, in some types of In foil measurements, such as ours, this additional A_s(high energy) is important and should be taken into account. On the other hand, it is seen that Eq. (4) is valid throughout the range of r over which we have measured.

(E) Boron Absorption Measurements

The above work on self-absorption gives a technique for correcting the activity of an indium foil to correspond to the 1.44-ev line, but provides little information concerning the high energy activity. In an effort to learn something of the character of this high energy indium cross section, distributions of indium foil activity *vs.* the distance r under two boron thicknesses were made (Table IV). These thicknesses of boron, 0.338 g/cm^2 and 1.334 g/cm^2, 88 percent B^{10}, were each sufficient to remove effectively the 1.44-ev line.

Interpretation of these distributions in a conclusive way turned out to be impossible since there is no theory, such as Eq. (4), applicable in the relevant detecting energy range, i.e., from perhaps 100 ev to 3 kev. However, it may be stated qualitatively that the high energy activity is not due to a single or narrow group of lines since the two boron covered distributions are not proportional to each other.

The authors are happy to acknowledge their appreciation to Dr. A. M. Weinberg and to Dr. G. Goertzel for numerous helpful theoretical discussions in connection with this experiment.